

---

## Organophosphate Ester Flame Retardants and Plasticizers in the Global Oceanic Atmosphere

Castro-Jimenez Javier <sup>1,2,\*</sup>, Gonzalez-Gaya Belen <sup>1,3</sup>, Pizarro Mariana <sup>1</sup>, Casal Paulo <sup>1</sup>,  
Pizarro-Alvarez Cristina <sup>1</sup>, Dachs Jordi <sup>1</sup>

<sup>1</sup> CSIC, Dept Environm Chem, Inst Environm Assessment & Water Res IDAEA, Jordi Girona 18-26, ES-08034 Barcelona, Spain.

<sup>2</sup> Univ Toulon & Var, Aix Marseille Univ, CNRS INSU, Mediterranean Inst Oceanog MIO UM 110,IRD, F-13288 Marseille, France.

<sup>3</sup> CSIC, Inst Organ Chem IQOG, Dept Instrumental Anal & Environm Chem, Juan Cierva 3, Madrid, Spain.

\* Corresponding author : Javier Castro-Jimenez, email address :

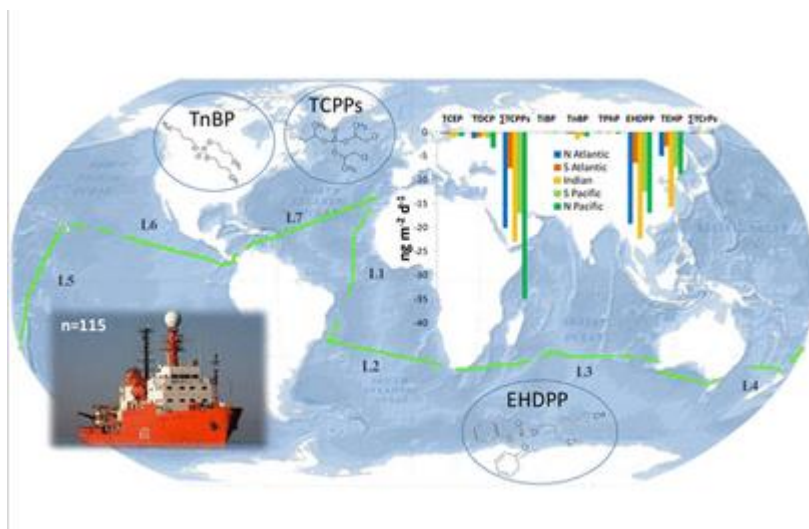
[javier.castro-jimenez@mio.osupytheas.fr](mailto:javier.castro-jimenez@mio.osupytheas.fr)

---

### Abstract :

Organophosphate esters (OPEs) are widely used as flame retardants and plasticizers and have been detected ubiquitously in the remote atmosphere. Fourteen OPEs were analyzed in 115 aerosol phase samples collected from the tropical and subtropical Atlantic, Pacific, and Indian Oceans during the MALASPINA circumnavigation campaign. OPEs were detected in all samples with concentrations ranging from 360 to 4400 pg m<sup>-3</sup> for the sum of compounds. No clear concentration trends were found between the Northern and Southern hemispheres. The pattern was generally dominated by tris(1-chloro-2-propyl) phosphate (TCPP), although tri-nbutyl phosphate (TnBP) had a predominant role in samples close to continents and in those influenced by air masses originating in continents. The dry deposition fluxes of aerosol phase Sigma 14OPE ranged from 4 to 140 ng m<sup>-2</sup> d<sup>-1</sup>. An estimation of the OPE gas phase concentration and gross absorption fluxes by using three different sets of physical chemical properties suggested that the atmosphere-ocean diffusive exchange of OPEs could be 2-3 orders of magnitude larger than dry deposition. The associated organic phosphorus inputs coming from diffusive OPE fluxes were estimated to potentially trigger up to 1.0% of the reported primary production in the most oligotrophic oceanic regions. However, the uncertainty associated with these calculations is high and mostly driven by the uncertainty of the physical chemical properties of OPEs. Further constraints of the physical chemical properties and fluxes of OPEs are urgently needed, in order to estimate their environmental fate and relevance as a diffusive source of new organic phosphorus to the ocean.

## Graphical abstract



## 43    **Introduction**

44

45    Organophosphorus flame retardants (PFRs) have been used as substitutes of  
46    polybrominated diphenyl ethers (PBDEs) after their almost-complete ban by the  
47    Stockholm convention on persistent organic pollutants (POPs) in 2009.<sup>1</sup> The shifting of  
48    the flame retardants market from PBDEs to PFRs has led to a rapid increase of the  
49    world-wide consumption of these chemicals. Organophosphate esters (OPEs) are a  
50    group of PFRs also used as plasticizers, and includes halogenated and non-halogenated  
51    compounds.<sup>2</sup> The annual global consumption of PFRs, including OPEs, reached ~ 300  
52    000 tonnes in 2011<sup>3</sup> and a 5% annual increase (average annual growth rate) is expected  
53    according to a recent market study.<sup>4</sup>

54    OPEs were thought to be degradable enough as to exhibit low persistency in the  
55    environment and low Long Range Atmospheric Transport (LRAT) potential. Estimates  
56    of half-life times in the environment are particularly short for the atmospheric gas  
57    phase.<sup>5</sup> In addition, OPEs were thought to elicit negligible hazardous effects in the  
58    environment as compared to PBDEs. However, last scientific evidences contradict these  
59    initial assumptions in an increasing number of cases. The fact that OPEs have been  
60    found in indoor and outdoor environments (in biotic and non-biotic compartments) in  
61    rural, urban and industrial areas,<sup>6</sup> but also in remote regions,<sup>7-9</sup> proves their multi-media  
62    global occurrence and high potential for LRAT, consistent with the latest reports  
63    highlighting the longer atmospheric half-lives for particle-bound OPEs.<sup>10</sup> Evidence of  
64    their environmental persistency, bioaccumulation and adverse effects in aquatic  
65    organisms and humans have also been reported.<sup>2,6,11-14</sup> These observations have raised  
66    awareness on their environmental fate and impacts as it already happened in the past for  
67    other POPs.

68

69 The open ocean constitutes an extensive and sensitive remote area of our planet  
70 providing early warning on global chemical pollution. OPEs enter the oceanic  
71 environment by atmospheric deposition like other semi-volatile organic contaminants  
72 (SVOCs),<sup>15-19</sup> even though oceanic transport may also be important for some OPEs.<sup>20</sup>  
73 Current investigations focusing on the atmospheric occurrence and loading of OPEs in  
74 these large remote oceanic regions have been undertaken by dedicated oceanographic  
75 campaigns usually covering only one or few of the sub-regions of the ocean/sea of  
76 interest, probably due to logistic and opportunistic limitations. The majority of the  
77 measurements have been performed in a number of marine regions from the Northern  
78 hemisphere (NH): i.e. Arctic Ocean,<sup>8,9,21</sup> North Pacific Ocean,<sup>21</sup> Sea of Japan,<sup>21</sup> China  
79 Sea,<sup>22,23</sup> North Sea,<sup>24</sup> Mediterranean and Black Seas<sup>25</sup> and the Philippine Sea.<sup>21</sup> A limited  
80 number of studies have been conducted in the Southern hemisphere (SH): i.e. Coral  
81 Sea,<sup>22</sup> Indian Ocean<sup>21</sup> and Southern Ocean.<sup>21,22</sup> In addition to the interest in quantifying  
82 the oceanic sink of OPEs and their ecotoxicological impact, OPEs are also a source of  
83 organic phosphorus for the most oligotrophic marine environments,<sup>25</sup> not yet quantified  
84 globally.

85 We report here results from a unique set of atmospheric samples collected during a 7-  
86 month circumnavigation campaign (MALASPINA 2010), covering the tropical and  
87 subtropical areas of the North and South Atlantic and Pacific Oceans, and the Indian  
88 Ocean. The main objectives of this study were: (1) to provide the first global assessment  
89 of the occurrence of OPEs in the tropical and subtropical oceanic atmosphere, and (2) to  
90 estimate their depositional fluxes to oceanic waters, and its associated organic  
91 phosphorus input to the oceans.

92

## 93 **Materials and Methods**

94 *Study region and sampling*

95

96 A total of 115 atmospheric samples were collected from December 2010 to July 2011 in  
97 seven consecutive transects (L1-L7, Figure S1) during the MALASPINA  
98 circumnavigation campaign on board of the RV Hespérides, encompassing all the  
99 tropical and temperate oceans between 35°N and 40°S. High volume air samplers  
100 (MCV, Barcelona, Spain), installed on the upper deck of the ship (above the bridge),  
101 were used to gather the atmospheric particle phase as explained elsewhere<sup>17, 19</sup> (Text  
102 S1). Briefly, the air was drawn through pre-combusted quartz fiber filters (QFFs) to  
103 collect aerosol-bound compounds (total suspended particles, TSP). The samplers were  
104 automatically stopped when wind was coming from the rear of the boat to avoid  
105 potential sample contamination from the ship emissions. The average sampling volume  
106 was of  $\sim 850 \text{ m}^3$  (details for all sampling events are reported in Table S1). Most of  
107 existing studies performed in marine environments report that OPEs are mainly found in  
108 the aerosol phase,<sup>21-25</sup> so we focussed on the aerosol samples as the analytical method  
109 had been optimized for the aerosol phase. Very recent measurements proved that most  
110 common OPEs can also exist in the atmospheric gas phase in a coastal site,<sup>26</sup> and  
111 modelling estimations seem to confirm their atmospheric gas-particle partitioning.<sup>27</sup>  
112 We processed 10 of the polyurethane foams used to sample the gas phase compounds,  
113 which were collected and analysed as explained elsewhere.<sup>19</sup> Few of the targeted OPEs  
114 could be detected and not for all samples with a high variability in surrogate recoveries  
115 (results not shown). Most probably, this was due to the fact that the sampling, extraction  
116 and fractionation methods had not been specifically optimized for OPEs in PUF  
117 samples, and thus gas phase analysis was not further pursued. Below we discuss OPE

118 gas phase concentrations calculated by gas-particle partitioning using reported estimates  
119 of the octanol-air partition coefficient ( $K_{OA}$ ).

120

#### 121 *Analysis*

122

123 Briefly, QFFs were spiked with Tri-n-butyl-d27 phosphate and Triphenyl-d15  
124 phosphate labelled standards and were Soxhlet extracted (24h). The extracts were rota-  
125 evaporated and fractionated on alumina columns as reported elsewhere.<sup>17,25</sup> (details in  
126 Text S2). OPEs were eluted in the second and third fraction with  
127 hexane/dichloromethane and dichloromethane/methanol mixtures, respectively. Extracts  
128 were then concentrated to 50 – 150  $\mu$ L under a gentle nitrogen flow. Prior to injection,  
129 labelled standards (Tri-n-propyl-d21 phosphate, and malathion-d7) were added to the  
130 extracts to be used as internal standards for quantification. OPE analysis was conducted  
131 by gas chromatography (Agilent 6890 Series GC) coupled with a mass spectrometer  
132 (Agilent 5973 MS) (GC-MS) operating in selected ion monitoring (SIM) and electron  
133 impact (EI, 70eV) mode and compounds were quantified by the internal standard  
134 procedure (Table S2 shows selected ions for detection and quantification for each  
135 compound). The injector temperature was set at 280 °C and the splitless mode was used.  
136 The separation was achieved in a 30m x 0.25mm i.d. x 0.25 $\mu$ m HP-5MS capillary  
137 column (Agilent J&W). The oven temperature was programmed from 90°C (holding  
138 time 1min) to 170°C at 8°C/min, to 250°C at 4°C/min, then to 300°C at 10°C/min  
139 (holding time 9min). The injection volume was of 2 $\mu$ l and the helium carrier gas flow  
140 was 1 ml min<sup>-1</sup>. The temperatures of the MS transfer line and the ion source were set at  
141 280 °C and 230 °C, respectively.

142 Samples were analysed for the following OPEs: Tris-(2-chloroethyl)phosphate (TCEP),  
143 Tris[2-chloro-1-(chloromethyl)ethyl]phosphate (TDCP), Tris- (1-chloro-2-  
144 propyl)phosphate (TCPPs, mix of isomers), Tri-iso-butyl phosphate (TiBP), Tri-n-butyl  
145 phosphate (TnBP), Triphenyl phosphate (TPhP), 2-Ethylhexyl diphenyl phosphate  
146 (EHDPP), Tri(2-ethylhexyl) phosphate (TEHP) and Tricresyl phosphate (TCrP, mix of  
147 isomers).

148

149 *Quality assurance /Quality control (QA/QC)*

150

151 The QA/QC procedures are detailed in Text S3. Summarizing, field and laboratory  
152 (procedural for sampling and analysis) blanks were collected and analysed concurrently  
153 with the samples. Blank values are reported in Table S3. Mean blank levels in the  
154 aerosol phase were in general very low ranging from 0 to 8% of sample values,  
155 depending on the sample and the compound, except for TPhP which reached a  
156 maximum of ~ 30% of the sample amount. However, this higher percentage is due to  
157 the fact that TPhP exhibited the lowest ambient levels, since the absolute blank (amount  
158 of chemical) was in the same range as other OPEs. Results were blank corrected by  
159 subtracting individual OPE total blank average levels (n=20) from the corresponding  
160 sample levels. Procedural blanks showed lower or similar levels to field blanks so no  
161 contamination of samples during sampling and storage occurred.

162 Standards (natives + labelled compounds) were introduced in the chromatographic  
163 sequence to evaluate possible variations on the detection conditions during the time of  
164 analyses. Chromatographic peaks of target compounds were only considered when their  
165 abundance was at least 3 times higher than the instrumental noise. Instrumental limits of

166 detection (LODs) (calculated as signal-to-noise ratio > 3) ranged from 0.06 to 0.6 pg m<sup>-3</sup>  
167 depending on the compound (Table S4). The method recovery (extraction-clean up-  
168 analysis) varied from 41 to 85 % (median values, Figure S2). Results were not corrected  
169 by recoveries. A clear chromatographic peak identification and quantification was  
170 feasible in all aerosol samples.

171 NIST SRM 2585 was analysed for target OPEs. This reference material is not certified  
172 for OPEs, however nine different laboratories have provided concentration of OPEs in  
173 this dust reference material, becoming a recommended quality control step.<sup>28</sup> The  
174 average results for five replicates (blank corrected) proved that the analysis of OPE  
175 using the described methodologies provided concentrations in good agreement with  
176 reported values for most OPEs (Figure S3). Deviations were found for EHDPP and  
177 TCrPs, only.

178

#### 179 *Data statistical analysis*

180

181 Since the data set was not normally distributed, non-parametric tests (Kruskal-Wallis  
182 and Wilcoxon rank-sum) were used in order to investigate significant differences  
183 among pollutant's levels. The effect of multiple comparisons was taken into account by  
184 applying the False Discovery Rate method. The software employed was STATA/SE  
185 12.1. Details are presented in Text S4, Table S5 and Figure S4.

186

## 187 **Results and discussion**

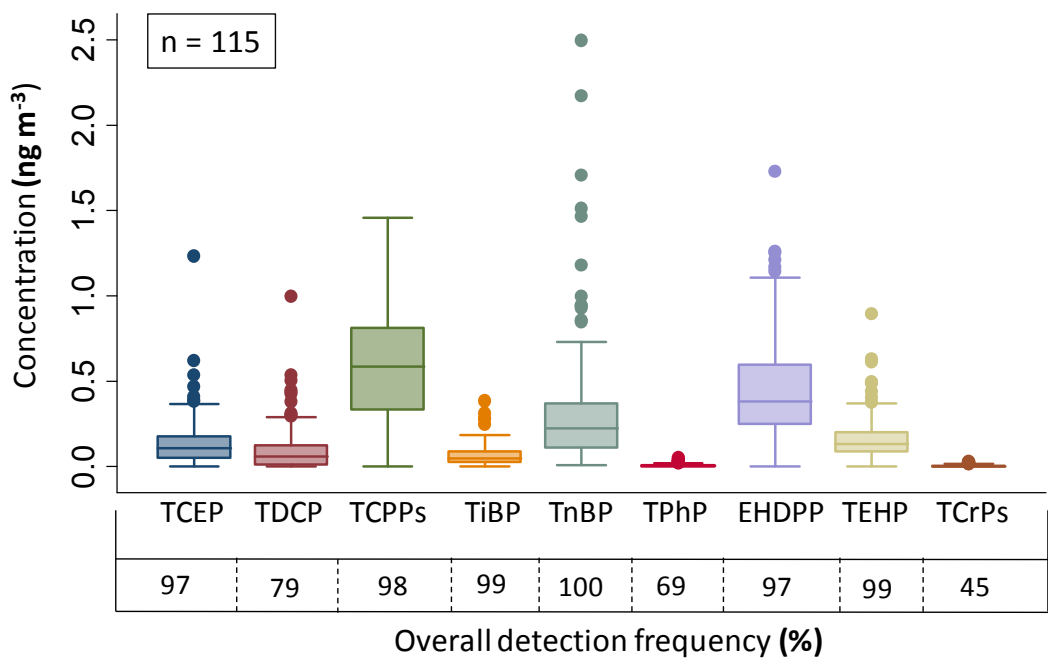
188

### 189 **Global atmospheric occurrence of OPEs**

190



191 *Detection frequency, atmospheric concentrations and pattern*  
192  
193 Most OPEs (i.e. TnBP, TiBP, TEHP, EHDPP, and the chlorinated TCPs and TCEP)  
194 were detected in the aerosol samples over the global tropical and subtropical oceans at  
195 considerably high frequencies (90 – 100%), confirming that these chemicals have  
196 equally reached remote waters from the NH and SH (Figure 1, Figure S5). However, the  
197 detected frequency of other OPEs like TPhP and TCrPs point to a reduced occurrence in  
198 the SH, in particular in the Indian Ocean, being only found in ~ 20 % (up to ~ 90% the  
199 in NH) and ~ 10% (up to ~ 80% in the NH) of the samples, respectively (Figure S5).  
200 Detection frequency of TDCP in the Indian Ocean was also low (detected in 44% of the  
201 samples collected in this region).



202  
203  
204 **Figure 1.** Box plots of atmospheric aerosol concentrations ( $\text{ng m}^{-3}$ ) of targeted OPEs  
205 across the tropical and subtropical regions of the major oceans (lines within the boxes

206 represent the median concentrations). Detection frequency (%) are numbers at the  
207 bottom squares. This comparison is shown in log-scale in Figure S6.

208

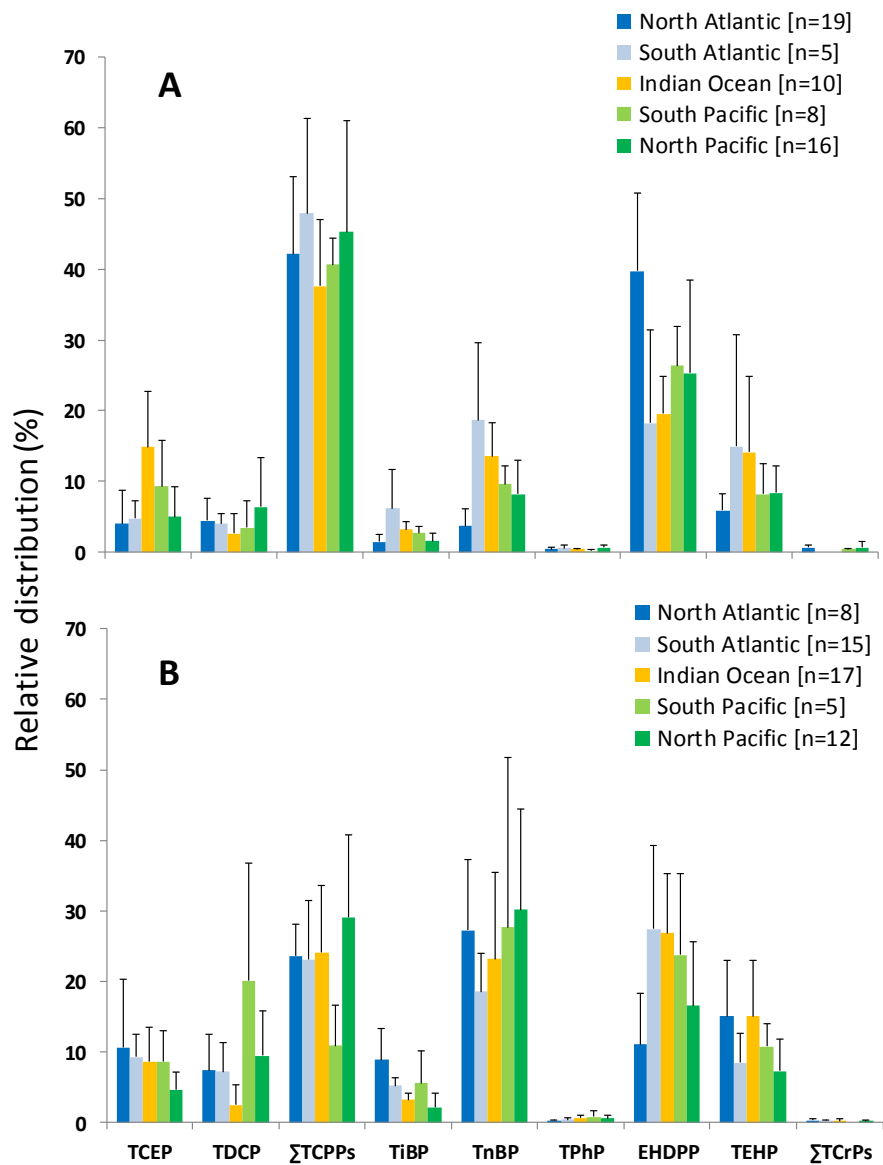
209  $\sum_{14}$ OPE aerosol phase concentrations varied from 360 to 4400  $\text{pg m}^{-3}$  (1800  $\text{pg m}^{-3}$ ,  
210 median) across the studied oceanic regions with TCPPs, EHDPP and TnBP dominating  
211 the OPE pattern with median concentrations of  $\sim 610$ , 390 and 220  $\text{pg m}^{-3}$ , respectively  
212 (Figure 1). Median, mean concentrations, and ranges in the various oceanic regions are  
213 presented in Table S6, whereas compound specific concentrations for all aerosol  
214 samples are reported in Table S7.

215

216 The atmospheric aerosol pattern of OPEs showed a general predominance of TCPPs in  
217 around half of the samples (Figure 2A), with TCPP contributing from  $38 \pm 9\%$  to  $48 \pm$   
218  $13\%$  of the  $\sum_{14}$ OPEs. EHDPP and TnBP were also abundant accounting from the  $18 \pm$   
219  $13\%$  to  $40 \pm 11\%$ , and from the  $4 \pm 2\%$  to  $19 \pm 11\%$  of the  $\sum_{14}$ OPEs, respectively.  
220 However, the other half of samples showed a higher contribution of TnBP (from  $19 \pm$   
221  $5\%$  to  $30 \pm 14\%$ , Figure 2B). This pattern was mostly observed in samples collected  
222 closer to the coast (like in Brazil area) or for which air masses (air mass back  
223 trajectories, BTs, calculated with HYSPLIT model<sup>29</sup>) showed a general continental  
224 influence (SW Mexico, NW Africa, S Africa and Madagascar and New Zealand)  
225 (Figure S7), but also in some SH regions with lower TCPP and higher TnBP  
226 abundances, respectively.

227 The dominant role of non-chlorinated OPEs, such as TnBP in the atmospheric pattern  
228 have been mostly reported in areas under the influence of suspected sources and in  
229 urbanized regions.<sup>9,20,21,30</sup> Conversely, the predominance of chlorinated OPEs, in  
230 particular TCPPs, in the atmospheric pattern has been previously reported for other

231 marine areas in the NH and SH, such as in the North Sea,<sup>24</sup> the Sea of Japan,<sup>21</sup> the  
232 Mediterranean and Black Seas,<sup>25</sup> the Indian and Southern oceans,<sup>21</sup> the East and South  
233 China Sea, and the Coral Sea.<sup>22,23</sup> Oceanic transport has been suggested to be important  
234 for chlorinated OPEs.<sup>20</sup>



235  
236 **Figure 2.** Relative predominance of OPEs in the global oceanic atmospheric aerosol.  
237 Columns show mean values + standard deviation of samples exhibiting a general TCPP  
238 predominance (A) and those showing higher contribution of TnBP (B) for each region.  
239

Most probably, the longer atmospheric half-lives of particle-bound TCPPs compared to TnBP<sup>9</sup> will result in a weathering of the atmospheric pattern during LRAT from the source areas to the open ocean. The atmospheric pattern weathering during LRAT has been described for other SVOCs such as dioxins<sup>18,31,32</sup>. The TCPP/TnBP ratio could provide information regarding the atmospheric weathering of OPE, and as an indicator of OPEs sources from land. In general, the smaller the ratio the higher the probability of proximity to sources (Table S8). For instance, the TCPP/TnBP ratio in this study ranged from 0.1 to 75 (Table S8), with the lowest ratios in the SH and in regions with air mass back trajectories influenced by land.

249

#### *Aerosol phase OPE spatial distribution*

251

Figure 3 shows the spatial distribution of the three most abundant OPEs. TCPPs and EHDPP follow a similar pattern with high levels in the Atlantic Ocean and an overall wide-spread distribution in both hemispheres. Contrarily, TnBP showed in general lower levels in the Atlantic but concentrations peaked in samples from the NE Pacific Ocean and NE Atlantic, with land influenced air mass BT (Figure S7). Differences in spatial distribution were also observed for the other OPEs (Figure S8). For instance, TDCP, TCEP, TPhP and TCrPs were generally less abundant in the SH and presented specific concentration peaks in some samples from the NH, whereas TEHP was found to be more abundant in the SH. The diverse spatial pattern of the individual OPEs may be the result of different sources for different individual compounds, and different physical-chemical properties and degradation pathways affecting their global cycling.

263

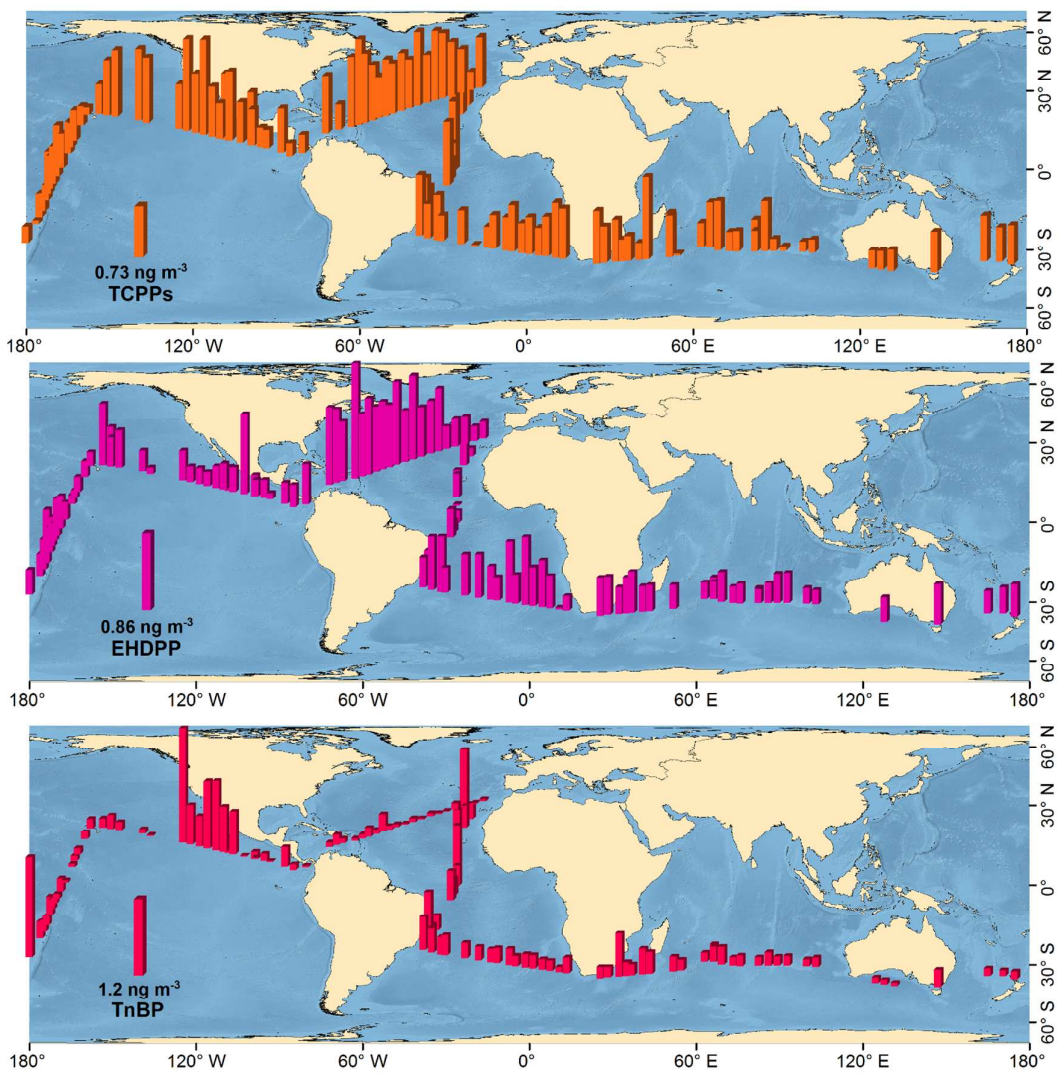


**Figure 3.** Spatial distribution of the most abundant OPEs (i.e TCPPs, EHDPP and TnBP) found in the global tropical and subtropical oceanic atmosphere.

Figure S9 shows the box plots for individual contaminant concentrations per oceanic region (as grouped in Figure S1). Statistically significant differences among oceanic regions (Kruskal-Wallis rank test,  $p = 0.0001 - 0.0046$ ) were found in the concentration of  $\sum_{14}\text{OPEs}$  and for all OPEs except for TEHP (Table S5). Contaminant concentrations (except for TEHP) were further compared by pairs of regions (Wilconxon rank-sum test) (Figure S4). The observed trends are far from being homogenous and are strongly

contaminant dependent. Not all contaminants exhibited consistent higher levels in one hemisphere over the other. Thus, TCEP, TiBP and TnBP exhibit higher levels (~3 fold, median values) in the South Atlantic than in the North Atlantic. However, only TiBP was higher in the South Pacific (~2 fold, median values) compared to the North Pacific (Table S6, Table S7) and TPhP concentration was higher in the North Pacific compared to the South (~2 fold, median values). The two regions showing more significant differences were the North Atlantic and the Indian ocean, with TDCP, EHDPP and TCrPs showing higher levels (2-5 fold, median values) in the North Atlantic, and the opposite trend for TCEP, TnBP and TPhP (1-2 fold higher levels in the Indian Ocean) was observed. This fact is highlighting the high compound specific variability in a given oceanic region and between the NH and SH. In general, the continental influence of the air masses gave rise to higher levels and changes in the atmospheric pattern (as discussed above). This situation mostly happened closer to the continental coasts at both hemispheres and in the Indian Ocean which is affected by northern air masses in the mid troposphere.<sup>17</sup> The influence of air masses is probably coupled with regionally dependent different use of individual OPE, and weathering during LRAT.

In addition, the variable amounts of the atmospheric TSP over the different oceanic regions affected the observed spatial patterns explaining part of the concentration variability. For example, when normalizing atmospheric concentrations by TSP (Table S9), the median  $\sum_{14}\text{OPEs}$  concentrations are similar for the North Atlantic ( $23.5 \text{ ug g}^{-1}_{\text{TSP}}$ ) and the Indian ocean ( $22.6 \text{ ug g}^{-1}_{\text{TSP}}$ ) (Figure S10 and Table S9), while the median volumetric concentrations was higher for the North Atlantic. High aerosol phase concentrations of semi-volatile organic pollutants such as dioxins and polycyclic aromatic hydrocarbons (PAHs) have also been observed in some oceanic gyres such as the Indian Ocean.<sup>17,18</sup>

Table 1 gathers existing data on OPE aerosol phase atmospheric concentrations from cruise measurements and remote coastal sites in various marine regions of the world. The majority of the studies have been performed in the NH. The present work complements those studies and fills important data gaps for some oceanic regions such as the open Atlantic and the South Pacific Oceans. Concentrations of halogenated OPE measured during the MALASPINA campaign in the NH are generally in the upper-end range of those reported for the most remote environments from this hemisphere (Table 1). Higher concentrations were found for some non-halogenated OPEs like TnBP and EHDPP, whereas TiBP and TCrPs were within the range of those levels in remote regions. The higher TnBP levels correspond mostly to the samples collected closer to the coast or with BT showing continental influence, as well as in the SH. Previous cruise measurements performed in the North Pacific Ocean<sup>21</sup> revealed generally lower OPE concentrations, except for TCEP and TPhP, with levels in the range of our measurements in North Pacific. However, even if both cruises sampled the same ocean, they had different geographical coverage. Regarding the SH, the concentrations measured during the MALASPINA expedition in the South Atlantic, Pacific and the Indian Oceans are generally higher than those reported for the most remote areas, in the southern Ocean<sup>21</sup> and near the Antarctic peninsula.<sup>22</sup> However, our concentrations compare well with the previously reported levels in the Indian Ocean.<sup>21</sup> The comparison of concentrations from different field studies should be made with caution as most previous studies did not report the concentrations from reference materials which limits the interlaboratory comparability (potential quantification bias), and used different sampling approaches including different deployment times (potential sampling bias due to OPE degradation). Sampling deployment times ranged from 12 to 24 hours in this work.

324 *Atmospheric dry deposition of OPEs to the global oceans*

325

326 Dry deposition fluxes ( $F_{DD}$ ,  $\text{ng m}^{-2} \text{d}^{-1}$ ) of OPEs were calculated as:

327

$$328 \quad F_{DD} = 864 v_d C_A \quad [1]$$

329

330 where  $C_A$  is the volumetric concentration of OPEs in the aerosol phase ( $\text{ng m}^{-3}$ ), and  $v_d$   
331 ( $\text{cm s}^{-1}$ ) is the deposition velocity of particles.  $v_d$  were predicted using the recently  
332 developed empirical parameterization derived from field measurements during the same  
333 MALASPINA circumnavigation cruise<sup>17</sup>:

334

$$335 \quad \text{Log}(v_d) = -0.261 \text{Log}(P_L) + 0.387 U_{10} * \text{Chl}_s - 3.082 \quad [2]$$

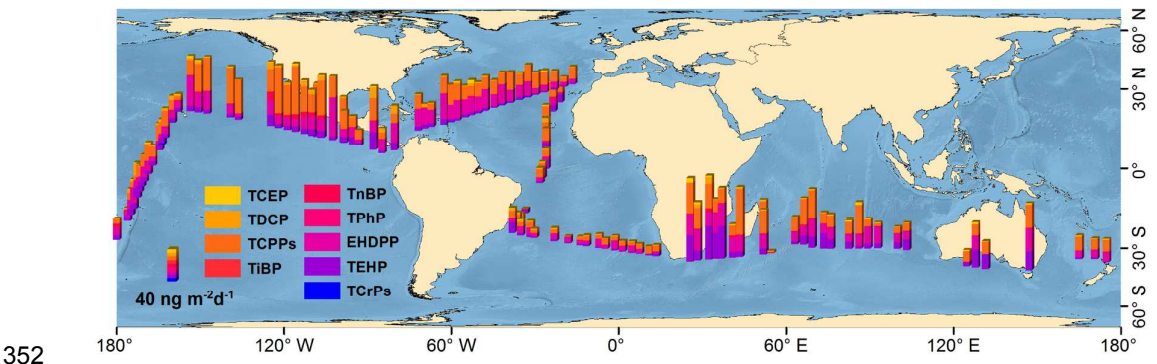
336

337 where  $U_{10}$  ( $\text{m s}^{-1}$ ) is the wind speed at 10 m over sea surface,  $\text{Chl}_s$  ( $\text{mg m}^{-3}$ ) is the  
338 chlorophyll a concentration in surface waters, and  $P_L$  (Pa) is the chemical vapor  
339 pressure of each OPE congener. This equation predicts higher depositional fluxes for  
340 the less volatile (more hydrophobic) chemicals, and higher depositional fluxes in those  
341 oceanic regions with higher wind speed, and higher phytoplankton biomass due to the  
342 formation of a surface microlayer enhancing the deposition of hydrophobic fine  
343 aerosols. <sup>33</sup>  $U_{10}$  and  $\text{Chl}_s$  were measured during the sampling campaign<sup>17</sup> and  $P_L$  values  
344 for OPEs were taken from literature<sup>34</sup>. The  $v_d$  calculated using equation [2] ranged from  
345 0.001 to 0.10  $\text{cm s}^{-1}$  depending on the oceanic region and compound (Figure S11).  
346 Figure 4 shows the OPE atmospheric dry deposition fluxes for each sampling point and  
347 compound. Median, mean and range of fluxes for single contaminant in each region are  
348 presented in Table S10, whereas values for all samples are shown in Table S11.



349 Atmospheric dry deposition fluxes of  $\sum_{14}\text{OPEs}$  across the major oceans of the Earth  
350 varied from 4 to 140  $\text{ng m}^{-2}\text{d}^{-1}$  (Figure 4, Table S11).

351



353 **Figure 4.** Atmospheric dry deposition fluxes ( $\text{ng m}^{-2} \text{d}^{-1}$ ) to surface waters of the  
354 tropical and subtropical regions of the major oceans

355

356 The atmospheric loading to marine waters is dominated by TCPPs, the most abundant  
357 OPE detected, with higher deposition fluxes in the North Pacific and Indian Oceans  
358 (higher  $v_d$  values calculated for these regions, Figure S11) reaching up to 35  $\text{ng m}^{-2}\text{d}^{-1}$   
359 (median value) in the North Pacific (Table S10). The annual dry deposition fluxes  
360 ( $\sum_{14}\text{OPEs}$ ) in the Pacific (considering a surface of  $1.7 \times 10^{14} \text{ m}^2$ ) and Indian (surface of  
361  $7.4 \times 10^{13} \text{ m}^2$ ) Oceans ranged from 1 to  $\sim 7 \text{ Kt y}^{-1}$  and from 0.1 to 4  $\text{Kt y}^{-1}$ , respectively.  
362 Generally lower annual deposition fluxes ( $0.2$  to  $2.5 \text{ Kt y}^{-1}$ ) were estimated for the  
363 Atlantic Ocean (surface of  $8.2 \times 10^{13} \text{ m}^2$ ). The surface waters of the tropical and  
364 subtropical oceans receive a resulting yearly integrated amount of  $\sim 2$  to 13  $\text{Kt y}^{-1}$  of  
365 OPEs (sum of 14 compounds) from the overlying atmosphere as a result of the dry  
366 deposition of particle-bound OPEs.

367

368 **OPEs as a source of new organic phosphorus (P) to the open ocean**

369

370 The anthropogenic impacts of OPEs, and other organophosphorus hazardous chemicals,  
371 may not be limited to toxic effects to wildlife and humans as reported so far, but also to  
372 the interactions with the natural phosphorous cycle<sup>25</sup>. Phosphorus is often a limiting  
373 nutrient in large oceanic regions,<sup>35,36</sup> but current estimates of phosphorus deposition to  
374 oceanic regions are mostly based on the assessment (measurements and model  
375 estimations) of inorganic phosphorus.<sup>37</sup> There is a raising interest to quantify the  
376 relevance and role of the organic phosphorus inputs (a fraction poorly characterized) on  
377 the oceanic biogeochemical cycles.<sup>37</sup>

378 The dry deposition of  $\sum_{14}\text{OPEs}$  given as organic phosphorus to the global oceans varied  
379 from 0.5 to 12 ngP m<sup>-2</sup> d<sup>-1</sup> (or from  $\sim 2 \times 10^{-7}$  to  $4 \times 10^{-6}$  gP m<sup>-2</sup> y<sup>-1</sup>). Assuming the  
380 phosphorus input coming from aerosol phase OPEs is bioavailable for planktonic  
381 organisms, it is estimated that it could trigger a primary productivity (using the Redfield  
382 ratio) accounting for around 0.001% of the primary productivity measured in the  
383 oligotrophic oceanic gyres during the MALASPINA campaign (100 - 600 mg C m<sup>-2</sup> d<sup>-1</sup>)  
384<sup>38</sup> or in other field studies (18 - 360 mg C m<sup>-2</sup> d<sup>-1</sup>)<sup>39</sup>.

385 The  $P_L$  range of the targeted OPEs in this study varied from 0.00002 Pa (TEHP) to 1.7  
386 Pa (TiBP). This  $P_L$  range is similar to that of other SVOCs with a well described  
387 atmospheric gas-particle partitioning such as polychlorinated biphenyls (PCBs), PAHs  
388 and some organochlorinated pesticides (OCPs)<sup>40,41</sup>. The issue of weather OPEs are  
389 found in the gas phase is extremely relevant for understanding and predicting their  
390 environmental fate. We know from other semi-volatile POPs that diffusive air-water  
391 exchange is the main depositional process. The diffusive atmospheric deposition (air-  
392 water exchange) of other SVOC with similar physical-chemical properties as OPEs,  
393 such as PAHs and PCBs, can be various orders of magnitude larger than the dry  
394 deposition fluxes in marine environments, in particular for the most volatile compounds

395 <sup>40, 41</sup>. In addition, this mechanism is the dominant pathway of SVOC loading to aquatic  
396 environments far from the coast due to a decrease in marine aerosol abundance in the  
397 open ocean <sup>40, 41</sup>.

398 Early works provided concentrations of OPEs in the gas phase over the North Sea, <sup>24</sup>  
399 with concentrations accounting from 15 to 65% of atmospheric OPEs. Recently, it has  
400 been reported that gas phase OPEs are predominant over a coastal site <sup>26</sup>, consistent  
401 with their predicted gas-particle partitioning from  $P_L$  and  $K_{OA}$ . <sup>27</sup> We estimated the gas  
402 phase concentrations of OPEs for each sampling event from the measured aerosol phase  
403 concentrations and  $K_{OA}$  <sup>42</sup>.  $K_{OA}$  values have been estimated for a wide range of OPEs<sup>5</sup>  
404 using three different approaches: the EPI Suite, SPARC and ABSOLV. The three  
405 estimates of the values of  $K_{OA}$  for OPEs are different by orders of magnitude <sup>5</sup>, leading  
406 to a very high variability of the predicted OPE gas phase concentrations. For example,  
407 the predicted median TCPP gas phase concentrations for the oceanic atmosphere were  
408 of  $\sim 46\ 000\ \text{pg m}^{-3}$  (EPI Suite),  $\sim 369\ 000\ \text{pg m}^{-3}$  (SPARC), and  $\sim 1500\ \text{pg m}^{-3}$   
409 (ABSOLV). The large variability in predictions is also true for other OPEs with lower  
410  $P_L$ . The predicted median gas phase concentrations of EHDPP were  $\sim 60\ \text{pg m}^{-3}$  (EPI  
411 Suite),  $\sim 300\ \text{pg m}^{-3}$  (SPARC),  $\sim 0.1\ \text{pg m}^{-3}$  (ABSOLV). Due to the lack of reports of gas  
412 phase concentrations for OPEs in most previous field studies, even in those where gas  
413 phase OPEs were targeted, one could think that the lower values predicted by the  
414 ABSOLV method would be close to the environmental levels. However, this cannot be  
415 assured until oceanic gas phase concentrations of OPEs are measured. In any case, these  
416 gas phase concentrations could be supporting important air-water diffusive fluxes of  
417 OPEs to the global oceans.

418 The diffusive gross absorption ( $F_{Abs}$ ,  $\text{ng m}^{-2} \text{d}^{-1}$ ) of gas phase OPEs was estimated by,  
419

$$F_{Abs} = k_{AW} \frac{C_G}{H'} \quad [3]$$

421

422 Where  $C_G$  is the gas phase concentrations ( $\text{ng m}^{-3}$ ),  $k_{AW}$  is the air-water mass transfer  
423 coefficient, estimated as previously reported<sup>40, 41</sup>, and  $H'$  is the dimensionless Henry's  
424 Law constant. We estimated  $F_{Abs}$  using the  $H'$  estimated from the EPI Suite, SPARC,  
425 and ABSOLV methods, which also show a large variability<sup>5</sup>.

426 The estimated mean gross diffusive fluxes of  $\Sigma_{14}\text{OPEs}$  were of  $60\,000 \text{ ng m}^{-2} \text{ d}^{-1}$  (EPI  
427 Suite),  $200 \text{ ng m}^{-2} \text{ d}^{-1}$  (SPARC), and  $6000 \text{ ng m}^{-2} \text{ d}^{-1}$  (ABSOLV). TCEP, TCPP, TiBP,  
428 and TnBP are the main OPEs contributing to this diffusive flux. The estimated average  
429 global inputs of P to the ocean due to gross diffusive air-water exchange were of  $6600$   
430  $\text{ngP m}^{-2} \text{ d}^{-1}$  (EPI Suite),  $24 \text{ ngP m}^{-2} \text{ d}^{-1}$  (SPARC), and  $620 \text{ ngP m}^{-2} \text{ d}^{-1}$  (ABSOLV). The  
431 estimated mean primary productivity that the diffusive air-water exchange of OPEs  
432 could trigger due to inputs of bioavailable P would be of  $0.3 \text{ mg C m}^{-2} \text{ d}^{-1}$  (EPI Suite),  
433  $0.001 \text{ mg C m}^{-2} \text{ d}^{-1}$  (SPARC), and  $0.03 \text{ mg C m}^{-2} \text{ d}^{-1}$  (ABSOLV). These diffusive inputs  
434 of P (from OPEs) account from 0.0002% to more than 1% of primary production in the  
435 oligotrophic oceans, and the upper-end estimates are one order of magnitude larger than  
436 phosphorus diffusive inputs previously considered by biogeochemical models<sup>37</sup>. It is  
437 noteworthy that this is a potential input of new (non-recycled) organic phosphorus to the  
438 ocean, but this input cannot be constrained until the uncertainty related to OPE's  
439 physical-chemical properties is significantly reduced.

440 Several studies have reported changes in primary production and chlorophyll a  
441 concentrations during the last century.<sup>43,44</sup> Environmental and climatic change can  
442 induce an increase or decrease of primary production due to a number of factors.<sup>43,44</sup>  
443 The figures obtained here for organic phosphorus inputs due to OPEs, even if their  
444 gaseous deposition fluxes have an uncertainty of orders of magnitude, suggest that these

445 chemicals, acting together with other anthropogenic pollutants containing P and N,  
446 could be triggering small perturbations of the regional/global oceanic primary  
447 production, and of comparable magnitude than those observed during the anthropocene.  
448 This would suggest another, yet neglected, interaction of the anthropogenic  
449 chemosphere with the other vectors of global change. Further work on the oceanic  
450 occurrence of OPEs, including waterborne long range transport, and determination of  
451 physical chemical properties of OPEs is urgently needed to constrain the uncertainty on  
452 their environmental fate and relevance.

453

454

## 455    **Acknowledgements**

456

457    This work was funded by the Spanish Ministry of Economy and Competitiveness  
458    (Circumnavigation Expedition Malaspina 2010: Global Change and Biodiversity  
459    Exploration of the Global Ocean. CSD2008-00077). CSIC and MAGRAMA are also  
460    acknowledged for additional financial support. J. Castro-Jiménez acknowledges the  
461    JAE-DOC contract from CSIC co-funded by the European Social Fund (ESF). BBVA  
462    Foundation is acknowledged for its economic support of the PhD fellow granted to B.  
463    González-Gaya. P. Casal and C. Pizarro acknowledge FPI and FPU fellowships from  
464    the Economy and Competitiveness Ministry of Spain. Thanks to Ana Maria Cabello,  
465    Pilar Rial, Prof. Marta Estrada, Prof. Mikel Latasa, Prof. Francisco Rodríguez, and Prof.  
466    Patrizija Mozetič for the Chlorophyll measurements during the Malaspina cruise. M.  
467    José Bleda is acknowledged for her contribution regarding the statistical analysis of  
468    data. Part of this research is also a contribution to the Labex OT-Med (no. ANR-11-  
469    LABX-0061) funded by the French Government “Investissements d’Avenir” (ANR)  
470    through the A\*MIDEX project (no ANR-11-IDEX-0001-02).

471

## 472    **Supporting information available**

473

474    Additional data on the sampling and analytical procedures, QA/QC, compound-by-  
475    compound atmospheric levels, spatial distribution and deposition fluxes are presented in  
476    this section. This information is available free of charge via the Internet at  
477    <http://pubs.acs.org/>

478

479 **References**

480 (1) Report of the Conference of the Parties of the Stockholm Convention on Persistent  
481 Organic Pollutants on the Work of Its Fourth Meeting; United Nations Environment  
482 Programme: Stockholm Convention on Persistent Organic Pollutants: Geneva, 2009; p p  
483 112.

484

485 (2) van der Veen, I.; de Boer, J. Phosphorus flame retardants: properties,  
486 production, environmental occurrence, toxicity and analysis. *Chemosphere* **2012**, *88*  
487 (10), 1119-1153.

488

489 (3) Flame retardants on-line: [http://www.flameretardants-](http://www.flameretardants-online.com/web/en/106/7ae3d32234954e28e661e506e284da7f.htm)  
490 [online.com/web/en/106/7ae3d32234954e28e661e506e284da7f.htm](http://www.flameretardants-online.com/web/en/106/7ae3d32234954e28e661e506e284da7f.htm) (Accessed  
491 23/11/2015)\

492

493 (4) Market Study: Flame retardants (3<sup>rd</sup> Edition) Ceresana, 2014.  
494 <http://www.ceresana.com/en/market-studies/additives/flame-retardants-new/> (Accessed  
495 23/11/2015)

496

497 (5) Zhang, X.; Sühling, R.; Serodio, D.; Bonnell, M.; Sundin, N.; Diamond, M.L. Novel  
498 flame retardants: Estimating the physical-chemical properties and environmental fate of  
499 94 halogenated and organophosphate PBDE replacements. *Chemosphere* **2016**, *144*,  
500 2401-2408.

501

502 (6) Wei, G-L.; Li, D-Q.; Zhuo, M-N.; Liao, Y-S.; Xie, Z-Y.; Guo, T-L.; Li, J-J., Zhang,  
503 S-Y.; Liang, Z-Q. Organophosphorus flame retardants and plasticizers: Sources,  
504 occurrence, toxicity and human exposure. *Environ. Pollut.* **2015**, *196*, 29-46.

505

506 (7) Marklund, A.; Andersson, B.; Haglund, P. Traffic as a source of organophosphorus  
507 flame retardants and plasticizers in snow. *Environ. Sci. Technol.* **2005**, *39* (10), 3555-  
508 3562.

509

510 (8) Green, N.; Schlabach, M.; Bakke, T.; Brevik, E.M.; Dye, C.; Herzke, D.; Huber, S.;  
511 Plosz, B.; Remberger, M.; Schøyen, M.; Uggerud, H.T; Vogelsang, C. Screening of  
512 selected metals and new organic contaminants 2007. Norwegian Pollution Control  
513 Authority, Report 1014/2008, 2008, ISBN- 978-82-577-5304-7.

514

515 (9) Salamova, A.; Hermanson, M. H.; Hites, R. A., Organophosphate and Halogenated  
516 Flame Retardants in Atmospheric Particles from a European Arctic Site. *Environ. Sci.*  
517 *Technol.* **2014**, *48*, 6133–6140.

518

519 (10) Liu, Y.; Liggio, J.; Harner, T.; Jantunen, L.; Shoeib, M.; Li, S-M. Heterogeneous  
520 OH Initiated Oxidation: A Possible Explanation for the Persistence of Organophosphate  
521 Flame Retardants in Air. *Environ. Sci. Technol.* **2014**, *48*, 1041–1048.

522

523

524 (11) European Chemical Agency (ECHA). 2008. Tris[2-Chloro-1-(Chloromethyl)ethyl]  
525 Phosphate (TDCP) CAS No.: 13674-87-8. EINECS No.: 237-159-2. Risk Assessment  
526 Report.



527

528 (12) European Chemical Agency (ECHA). 2009. Member State Committee support  
529 document for the identification of Tris (2-chloroethyl) phosphate as a substance of very  
530 high concern because of its CMR properties.

531

532 (13) Wang, Q.; Lai, N.L-S.; Wang, X.; Guo, Y.; Lam, P. K-S.; Lam, J. C-W.; Zhou, B.  
533 Bioconcentration and Transfer of the Organophorous Flame Retardant 1,3-Dichloro-2-  
534 propyl Phosphate Causes Thyroid Endocrine Disruption and Developmental  
535 Neurotoxicity in Zebrafish Larvae. *Environ. Sci. Technol.* **2015**, *49*, 5123–5132.

536

537 (14) Wang, Q.; Lam, J. C-W.; Han, J.; Wang, X.; Guo, Y.; Lam, P. K-S.; Zhou, B.  
538 Developmental exposure to the organophosphorus flame retardant tris(1,3-dichloro-2-  
539 propyl) phosphate: Estrogenic activity, endocrine disruption and reproductive effects on  
540 zebrafish. *Aquatic Toxicol.* **2015**, *160*, 163–171.

541

542 (15) Jurado, E.; Jaward, F.M.; Lohmann, R.; Jones, K.C.; Simó, R.; Dachs, J.  
543 Atmospheric dry deposition of persistent organic pollutants to the Atlantic and  
544 inferences for the global oceans. *Environ. Sci. Technol.* **2004**, *38* (21), 5505-5513.

545

546 (16) Jurado, E.; Jaward, F.M.; Lohmann, R.; Jones, K.C.; Simó, R.; Dachs, J. Wet  
547 deposition of persistent organic pollutants to the global oceans. *Environ. Sci. Technol.*  
548 **2005**, *39* (8), 2426–2435.

549

- 550 (17) González-Gaya, B.; Zúñiga-Rival, J.; Ojeda, M-J. Jiménez, B.; Dachs, J. Field  
551 Measurements of the Atmospheric Dry Deposition Fluxes and Velocities of Polycyclic  
552 Aromatic Hydrocarbons to the Global Oceans. *Environ. Sci. Technol.* **2014**, 48,  
553 5583–5592.
- 554
- 555 (18) Morales, L.; Dachs, J.; González-Gaya, B.; Hernán, G.; Ábalos, M.; Abad E.  
556 Background Concentrations of Polychlorinated Dibenzo-p-Dioxins, Dibenzofurans,  
557 and Biphenyls in the Global Oceanic Atmosphere. *Environ. Sci. Technol.* **2014**, 48,  
558 10198–10207.
- 559
- 560 (19) González-Gaya, B.; Fernández-Pinos, M-C.; Morales, L.; Méjanelle, L.; Abad, E.;  
561 Piña, B.; Duarte, C.M.; Jiménez, B.; Dachs, J. High atmosphere–ocean exchange of  
562 semivolatile aromatic hydrocarbons. *Nature Geosci.* **2016**, 9, 438–442
- 563
- 564 (20) Sühling, R.; Diamond, M.L.; Scheringer, M.; Wong, F.; Pućko, M.; Stern, G.; Burt,  
565 A.; Hung, H.; Fellin, P.; Li, H.; Jantunen, L.M. Organophosphate Esters in Canadian  
566 Arctic Air: Occurrence, Levels and Trends. *Environ. Sci. Technol.* **2016**, 50, 7409-7415.
- 567
- 568 (21) Möller, A.; Sturm, R.; Xie, Z.; Cai, M.; He, J.; Ebinghaus, R. Organophosphorus  
569 flame retardants and plasticizers in airborne particles over the Northern Pacific and  
570 Indian Ocean towards the polar regions: Evidence for global occurrence. *Environ. Sci.*  
571 *Technol.* **2012**, 46 (6), 3127-3134.
- 572

- 573 (22) Cheng, W.; Xie, Z.; Blais, J.M.; Zhang, P.; Li, M.; Yang, C.; Huang, W.; Ding, R.;  
574 Sun, L. Organophosphorus esters in the oceans and possible relation with ocean gyres.  
575 *Environ. Pollut.* **2013**, 180, 159-164  
576
- 577 (23) Lai, S.; Xie, Z.; Song, T.; Tang, J.; Zhang, Y.; Mi, W.; Peng, J.; Zhao, Y.; Zou, S.;  
578 Ebinghaus, R. Occurrence and dry deposition of organophosphate esters in atmospheric  
579 particles over the northern South China Sea. *Chemosphere* **2015**, 127, 195–200  
580
- 581 (24) Möller, A.; Xie, Z.; Caba, C.; Sturm, R.; Ebinghaus, R. Organophosphorus flame  
582 retardants and plasticizers in the atmosphere of the North Sea. *Environ. Pollut.* **2011**,  
583 159 (12), 3660-3665.  
584
- 585 (25) Castro-Jiménez, J.; Berrojalbiz, N.; Pizarro, M.; Dachs, J. Organophosphate Ester  
586 (OPE) Flame Retardants and Plasticizers in the Open Mediterranean and Black Seas  
587 Atmosphere. *Environ. Sci. Technol.* **2014**, 48, 3203-3209.  
588
- 589 (26) Wolschke, H.; Sühling, R.; Mi, W.; Möller, A.; Xie, Z.; Ebinghaus, R.  
590 Atmospheric occurrence and fate of organophosphorus flame retardants and plasticizer  
591 at the German coast. *Atmos. Environ.* **2016**, 137, 1-5.  
592
- 593 (27) Sühling, R.; Wolschke, H.; Diamond, M.L.; Jantunen, L.M.; Scheringer, M.  
594 Distribution of Organophosphate Esters between the Gas and Particle Phase—Model  
595 Predictions vs Measured Data. *Environ. Sci. Technol.* **2016**, 50, 6644–6651  
596

- 597 (28) Fan, X.; Kubwabo, C.; Rasmussen, P.E.; Wu, F. Simultaneous determination of  
598 thirteen organophosphate esters in settled indoor house dust and a comparison between  
599 two sampling techniques. *Sci. Total Environ.* **2014**, 491-492, 80–86.
- 600
- 601 (29) Draxler, R.R.; Rolph, G.D. 2011. HYSPLIT (HYbrid Single-Particle Lagrangian  
602 Integrated Trajectory) Model access via NOAA ARL READY Website;  
603 <http://ready.arl.noaa.gov/HYSPLIT.php>. NOAA Air Resources Laboratory, Silver  
604 Spring, MD.
- 605
- 606 (30) Salamova, A.; Ma, Y.; Venter, M.; Hites, R.A High levels of organophosphate  
607 flame retardants in the Great Lakes atmosphere. *Environ. Sci. Technol. Lett.*, **2014**, 1  
608 (1), 8-14.
- 609
- 610 (31) Castro-Jiménez, J; Eisenreich, S.J.; Ghiani, M.; Mariani, G.; Skejo, H.; Umlauf, G.;  
611 Wollgast, J.; Zaldívar, J.M.; Berrojalbiz, N.; Reuter, H.I; Dachs, J. Atmospheric  
612 occurrence and deposition of polychlorinated dibenzo-p-dioxins and dibenzofurans  
613 (PCDD/Fs) in the open Mediterranean Sea. *Environ. Sci. Technol.* **2010**, 44 (14), 5456-  
614 5463.
- 615
- 616 (32) Lohmann, R.; Jones, K. C. Dioxins and furans in air and deposition: a review of  
617 levels, behaviour and processes. *Sci. Total Environ.* **1998**, 219, 53–81.
- 618
- 619 (33) del Vento, S.; Dachs, J. Influence of the surface microlayer on atmospheric  
620 deposition of aerosols and polycyclic aromatic hydrocarbons. *Atmos. Environ.* 2007, 41,  
621 4920–4930.

622

623 (34) Brommer, S.; Jantunen, L.M.; Bidleman, T.F.; Harrad, S.; Diamond M.L.  
624 Determination of Vapor Pressures for Organophosphate Esters. *J. Chem. Eng. Data*,  
625 **2014**, *59*, 1441–1447

626

627 (35) Falkowski, P.G.; Barber, R.T.; Smetacek, V. Biogeochemical Controls and  
628 Feedbacks on Ocean Primary Production. *Science*, **1998**, *281*, 200–206.

629

630 (36) Mather, R.L.; Reynolds, S.E.; Wolff, G.A.; Williams, R.G.; Torres-Valdes, S.;  
631 Woodward, E.M.S.; Landolfi, A.; Pan, X.; Sanders, R.; Achterberg, E.P. Phosphorus  
632 cycling in the North and South Atlantic Ocean subtropical gyres. *Nature Geosciences*  
633 **2008**, *1*, 439–443.

634

635 (37) Kanakidou, M. Duce R.A., Prospero J.M., Baker A.R., Benitez-Nelson C.,  
636 Dentener F.J., Hunter K.A., Liss P.S., Mahowald N., Okin G.S., Sarin M., Tsigaridis K.,  
637 Uematsu M., Zamora L.M. and Zhu T.14 Atmospheric fluxes of organic N and P to the  
638 global ocean. *Global Biogeochem. Cy.* **2012**, *26* (3), GB3026.

639

640 (38) Pinedo-González, P.; West, A.J.; Tovar-Sánchez, A.; Duarte, C.M.; Marañón, E.;  
641 Cermeño, P.; González, N.; Sobrino, C.; Huete-Ortega M.; Fernández, A.; López-  
642 Sandoval, D.C.; Vidal, M.; Blasco, D.; Estrada, M.; Sañudo-Wilhelmy, S.A. Surface  
643 distribution of dissolved trace metals in the oligotrophic ocean and their influence on  
644 phytoplankton biomass and productivity. *Global Biogeochem. Cycles*, **2015**, *29*, 1763–  
645 1781, doi:10.1002/2015GB005149.

646

- 647 (39) Marañón, E.; Behrenfeld, M.J.; González, N.; Mouriño, B.; Zubkov, M.V. High  
648 variability of primary production in oligotrophic waters of the Atlantic Ocean:  
649 uncoupling from phytoplankton biomass and size structure. *Mar Ecol Prog Ser.* **2003**,  
650 257, 1-11.
- 651
- 652 (40) Castro-Jiménez, J.; Berrojalbiz, N.; Wollgast, J.; Dachs, J. Polycyclic aromatic  
653 hydrocarbons (PAHs) in the Mediterranean Sea: atmospheric occurrence, deposition and  
654 decoupling with settling fluxes in the water column. *Environ. Pollut.* **2012**, 166, 40-47.
- 655
- 656 (41) Berrojalbiz, N.; Castro-Jiménez, J.; Mariani, G.; Wollgast, J.; Hanke, G.; Dachs J.  
657 Atmospheric occurrence, transport and deposition of polychlorinated biphenyls and  
658 hexachlorobenzene in the Mediterranean and Black seas. *Atmos. Chem. Phys.* **2014**, 14,  
659 8947-8959.
- 660
- 661 (42) Finizio, A.; Mackay, D.; Bidleman, T.; Harner, T. Octanol-air partition coefficient  
662 as a predictor of partitioning of semi-volatile organic chemicals to aerosols. *Atmos.*  
663 *Environ.* **1997**, 31, 2289-2296.
- 664
- 665 (43) Henson, S. A; Sarmiento, J. L.; Dunne, J.P.; Bopp, L.; Lima, I.; Doney, S.C.; John,  
666 J.;Beaulieu, C Detection of anthropogenic climate change in satellite records of ocean  
667 chlorophyll and productivity. *Biogeosciences* **2010**, 7, 621-640.
- 668
- 669 (44) Boyce, D. G., Lewis, M. R. & Worm, B. Global phytoplankton decline over the  
670 past century. *Nature* **466**, 591-596.
- 671

672 **Table 1.** Compilation of existing measurements of OPE atmospheric levels (aerosol concentrations except where otherwise indicated) in different  
673 oceanic regions of the world. Median concentrations and range (in brackets) are shown for this study.  
674

	Sampling	Location type	Date	Compounds, $pg\ m^{-3}$								
				TCEP	TDCP	$\Sigma$ TCPPs	TiBP	TnBP	TPhP	EHDPP	TEHP	$\Sigma$ TCrPs
<i>Northern Hemisphere</i>												
Arctic Ocean <sup>20</sup>	Cruise	Open sea	2007-2013	n.d. - 856	n.d. - 13	n.d. - 660	n.r.	n.d. - 97	n.d. - 1930	n.d. - 11	n.d. - 7.5	n.d. - 12 <sup>(b)</sup>
Resolute Bay & Alert (Canada, Arctic) <sup>20</sup>	Remote	Coastal site	2008-2009, 2012	n.d. - 430	n.d. - 46	n.d. - 276	n.r.	n.d. - 2340	1.2 - 96	n.d. - 40	n.r.	n.d. - 1.7 <sup>(c)</sup>
Arctic Ocean <sup>21</sup>	Cruise	Open sea	Jun-September 2010	126-585	n.d. - 5	85 - 530	16 - 35	n.d - 36	10 - 60	n.r.	n.d. - 6	n.r.
Ny-Alesund (Svalbard, Arctic) <sup>7</sup>	Remote	Coastal site	Jun-September 2007	<200 - 270	87 - 250	<200 - 330	<10 - 140	<200	<50	<200 - 260	n.r.	n.r.
Longyearbyen (Svalbard, Arctic) <sup>9</sup>	Remote	Coastal site	September 2012-May 2013	40 - 60	2 - 294	10 - 186	n.r.	6 - 1000	1 - 50	6 - 300	1 - 40	n.r.
North Atlantic Ocean <sup>This study</sup>	Cruise	Open sea	Dec 2010, Jun-Jul 2011	50 [n.d.-1230]	80 [n.d.-425]	770 [n.d.-1310]	40 [5-380]	90 [10-1700]	10 [n.d.-50]	780 [20-1730]	140 [60 - 490]	10 [n.d. - 30]
North Pacific Ocean <sup>21</sup>	Cruise	Open sea	Jun-September 2010	160 - 280	5 - 8	98 - 270	14 - 20	6 - 14	9 - 24	n.r.	1 - 12	n.r.
North Pacific Ocean <sup>This study</sup>	Cruise	Open sea	May-Jun 2011	80 [n.d.-310]	90 [n.d.-500]	640 [100-1460]	30 [3-100]	170 [20-2500]	10 [n.d.-34]	320 [100-1210]	110 [60-380]	5 [n.d.-30]
Sea of Japan <sup>21</sup>	Cruise	Open sea	Jun-September 2010	237 - 1960	16 - 52	130 - 620	10 - 63	10 - 33	25 - 97	n.r.	5 - 38	n.r.
East China Sea <sup>22</sup>	Cruise	Open sea	October 2009-March 2010	134	828	9	n.r.	n.r.	n.r.	n.r.	n.r.	n.r.
South China Sea <sup>23</sup>	Curise	Open sea	September-October 2013	14 - 110	1 - 4	15 - 38	1 - 4	1 - 5	3 - 16	n.r.	2 - 16	n.r.
North Sea <sup>24 (a)</sup>	Cruise	Open sea	March, May, July 2010	6 - 100	7 - 78	30 - 1200	n.d. - 150	n.d. - 150	4 - 150	n.r.	n.d. - 30	n.r.
Mediterranean Sea <sup>25</sup>	Cruise	Open sea	Jun 2006, May 2007	70 - 854	n.d. - 460	126 - 2340	4 - 650	56 - 600	n.d. - 80	n.d. - 834	56 - 307	n.d. - 128
Black Sea <sup>25</sup>	Cruise	Open sea	Jun 2006, May 2007	300 - 2420	n.d. - 97	540 - 2720	66 - 190	200 - 370	3 - 40	n.d. - 310	36 - 190	n.d. - 73
Philippine Sea <sup>21</sup>	Cruise	Open sea	November 2010- March 2011	20 - 156	50 - 780	22 - 410	10 - 23	10 - 100	n.d. - 155	n.r.	6 - 92	n.r.
<i>Southern Hemisphere</i>												
South Atlantic <sup>This study</sup>	Cruise	Open sea	Jan-Feb 2011	150 [10-540]	130 [n.d.-540]	570 [20-980]	100 [30-280]	330 [120-1180]	10 [n.d.-25]	500 [n.d.-1020]	160 [50-890]	9 [n.d. - 20]
South Pacific <sup>This study</sup>	Cruise	Open sea	Feb-April 2011	140 [34-370]	60 [n.d.-1000]	530 [50-800]	50 [15-160]	200 [50-2170]	4 [n.d.-40]	400 [260-800]	160 [40-350]	6 [n.d.-8]
Coral Sea <sup>22</sup>	Cruise	Open sea	October 2009-March 2010	88	370	7	n.r.	n.r.	n.r.	n.r.	n.r.	n.r.
Indian Ocean <sup>21</sup>	Cruise	Open sea	November 2010- March 2011	46 - 570	n.d. - 220	37 - 550	7 - 96	7 - 75	n.d. - 74	n.r.	4 - 50	n.r.
Indian Ocean <sup>This study</sup>	Cruise	Open sea	Feb-March 2011	100 [50-620]	20 [n.d.-290]	370 [30-1250]	40 [n.d.-110]	230 [70-940]	8 [n.d.-12]	370 [n.d.-630]	180 [n.d.-630]	2 [n.d. - 5]
Southern Ocean <sup>21</sup>	Cruise	Open sea	November 2010- March 2011	74	80	55	16	14	20	n.r.	7	n.r.
Near Antartic Peninsula <sup>22</sup>	Cruise	Open sea	October 2009-March 2010	40	76	4 <sup>a</sup>	n.r.	n.r.	n.r.	n.r.	n.r.	n.r.

n.r. = not reported; (a) atmospheric concentrations correspond to the sum of gas+particle phases, (b) three TCrP isomers analyzed, (c) two TCrP isomers analyzed

675  
676